Instability of Bose–Einstein condensates in tilted lattices with time-periodical modulation



2010 J. Phys. B: At. Mol. Opt. Phys. 43 205307

(http://iopscience.iop.org/0953-4075/43/20/205307)

IOP Publishing Journal of Physics B: Atomic, Molecular and Optical Physics

J. Phys. B: At. Mol. Opt. Phys. **43** (2010) 205307 (7pp) doi:10.1088/0953-4075/43/20/205307

# Instability of Bose–Einstein condensates in tilted lattices with time-periodical modulation

**Ning-Ju Hui, Xiao-Qiang Xu and You-Quan Li**

Zhejiang Institute of Modern Physics and Department of Physics, Zhejiang University, Hangzhou 310027, People's Republic of China

E-mail: njhui@hbar.zju.edu.cn

Received 20 April 2010, in final form 15 August 2010
Published 5 October 2010
Online at stacks.iop.org/JPhysB/43/205307

**Abstract**

We study the dynamical stability of Bose–Einstein condensates in an optical lattice with a time-periodic modulation potential and a constant acceleration force simultaneously. We derive the explicit expressions of quasienergies and obtain the stability diagrams of the ground state in parameter spaces. For integer and non-integer (rational) ratios of the acceleration force to the modulation frequency, different dependence relationships of the critical interaction strength on the modulation amplitude are observed. Our results are expected to help experimentalists to determine parameter regions as required.

(Some figures in this article are in colour only in the electronic version)

## 1. Introduction

Since Bose–Einstein condensation (BEC) of dilute gases of alkali atoms was realized in 1995 [1–3], much attention has been paid to ultracold atomic systems in various configurations, such as optical lattices which are formed by counter-propagating off-resonance laser beams. Due to the flexibility of the system, the famous Mott-insulator–superfluid transition of BEC in optical lattices has been observed and studied [4, 5]. Dynamically, there are also many interesting phenomena, such as resonant tunnelling [6]. In the limit of vanishing particle interactions, e.g. in dilute bosonic gases, the system may exhibit Bloch oscillation [7, 8], similar to the behaviour of a single electron in a crystalline field of solids. For the case of condensates in periodic potentials, when its velocity is larger than the sound velocity, energetic (Landau) instability may dissipate the condensates [9]. On the other hand, the nonlinear scattering process between atoms may cause dynamical (modulational) instability [10] amplifying the oscillation behaviour [11], for which small deviations grow exponentially with time.

Dynamical stability, which describes whether the system remains stable or not during its time evolution, is our concern in this paper. We are interested in the dynamical response of BEC in modulated optical lattices. We note that the dynamical stability of the BEC system in optical lattices modulated by a time-periodic potential has been investigated both experimentally [12] and theoretically [13]. Also, the dynamical stability of the condensates in tilted optical lattices taking into account the effect of a constant acceleration force has attracted much attention [14–16]. Recently, BEC in tilted time-periodically modulated lattices formed by both a time-periodic modulation potential and a constant acceleration force was realized experimentally [17]. We focus on the dynamical stability of the above system to which less attention has been paid, and aim to determine the influence of the interparticle interactions.

The paper is organized as follows. In section 2, we describe our modulated optical lattice system with a modified Bose–Hubbard Hamiltonian (BHH) [18, 19]. In the mean-field approximation we derive the time-evolution equations and obtain explicit solutions. In order to determine the dynamical stability of the system, we adopt an ansatz [13, 15]. Based on the Floquet theorem, the quasienergy analysis, which is strongly related to the dynamical stability, is given in section 3. Two specific cases, integer and non-integer resonances, are considered. We also discuss the main features of the dynamical stability for both cases in section 4, including the comparison with experimental data. A summary with brief discussion is given in section 5.

 

## 2. Model and method

We consider ultracold bosonic gases in a one-dimensional optical lattice modulated by both a time-periodic potential and a constant external acceleration force simultaneously. To model such a system, we need to include the external modulation terms in the typical BHH, i.e.

$$\hat{H} = -J\sum_{\langle m,n\rangle}\left(\hat{a}_m^\dagger\hat{a}_n + \hat{a}_n^\dagger\hat{a}_m\right) + \frac{U}{2}\sum_m \hat{a}_m^\dagger\hat{a}_m^\dagger\hat{a}_m\hat{a}_m + [K\cos(\omega t) + d]\sum_m m\hat{n}_m. \tag{1}$$

Here, $\hat{a}_m\left(\hat{a}_m^\dagger\right)$ annihilates (creates) a boson at the $m$th lattice site and $\hat{n}_m = \hat{a}_m^\dagger\hat{a}_m$ is the particle number operator correspondingly. $J$ describes the tunnelling strength between adjacent sites which are indicated by the subscript $\langle m, n\rangle$. $U$ refers to the on-site interaction between atoms. $K$ and $\omega$ denote the amplitude and frequency of the time-periodic modulation potential, respectively, while $d$ stands for the constant acceleration force.

The dynamical properties of our system can be obtained by studying the Heisenberg equations of motion for $\hat{a}_m$. Provided that the particle number of atoms on each site is large enough, we can safely adopt the mean-field approach (MFA) [10, 15], which is very effective in providing predictions for the dynamic properties of the trapped bosons, to replace these operators with their expectation values, e.g., $\alpha_m = \langle\hat{a}_m\rangle/\sqrt{N_L}$, where $N_L$ is the average number of atoms per site. Then the time-evolution equations for $\alpha_m$ are expressed as

$$\mathrm{i}\frac{\partial\alpha_m}{\partial t} = -J(\alpha_{m+1} + \alpha_{m-1}) + g|\alpha_m|^2\alpha_m + [K\cos(\omega t) + d]m\alpha_m, \tag{2}$$

where the natural unit $\hbar = 1$ is taken and $g = N_L U$ denotes the normalized atomic interaction. Equations (2) are also regarded as discretized Gross–Pitaevskii (GP) equations. Additionally, the particle number conservation $\sum_m \hat{a}_m^\dagger\hat{a}_m = N$ gives $\sum_m |\alpha_m|^2 = L$, where $N$ and $L$ are the total numbers of atoms and optical lattice sites respectively and their ratio is $N_L$, i.e. $N_L = N/L$.

In the interaction-free case, i.e. $g = 0$, equations (2) describe the single-particle dynamics whose analytical solutions can be explicitly derived through the gauge transformation [16]

$$\alpha_m(t) \to \exp\left[-\mathrm{i}m\left(\mathrm{d}t + \frac{K}{\omega}\sin(\omega t)\right)\right]\tilde{\alpha}_m(t). \tag{3}$$

Then equations (2) become

$$\mathrm{i}\frac{\partial\tilde{\alpha}_m}{\partial t} = -J(\mathrm{e}^{-\mathrm{i}D(t)}\tilde{\alpha}_{m+1} + \mathrm{e}^{\mathrm{i}D(t)}\tilde{\alpha}_{m-1}), \tag{4}$$

where $D(t) = \mathrm{d}t + K/\omega\sin(\omega t)$. Because the translation symmetry is retrieved back in the above equation, we can impose the spatial periodic boundary conditions, i.e. $\tilde{\alpha}_m(t) = \tilde{\alpha}_{L+m}(t)$. The corresponding semi-classical Hamiltonian now reads

$$H(t) = -J\sum_m(\mathrm{e}^{-\mathrm{i}D(t)}\tilde{\alpha}_m^*\tilde{\alpha}_{m+1} + \mathrm{e}^{\mathrm{i}D(t)}\tilde{\alpha}_{m+1}^*\tilde{\alpha}_m). \tag{5}$$

The Bloch-wave representation is desirable in order to obtain the solutions for $\tilde{\alpha}_m$,

$$\tilde{\alpha}_m = L^{-1/2}\sum_k \mathrm{e}^{\mathrm{i}km}b_k, \tag{6}$$

where $k = 2\pi n/L$ is the quasimomentum ($-\pi \leqslant k < \pi$), $n = 0, \pm1, \ldots, \pm(L-1)/2$ for odd $L$, while $n = 0, \pm1, \ldots, \pm L/2$ for even $L$. Then the evolution equations of $b_k$ take the following simple form:

$$\mathrm{i}\frac{\partial b_k}{\partial t} = -2J\cos\left[k - \mathrm{d}t - \frac{K}{\omega}\sin(\omega t)\right]b_k, \tag{7}$$

whose solutions can be explicitly expressed as

$$b_k(t) = b_k(0)\exp\left\{\mathrm{i}2J\left[\cos(k)S(t) - \sin(k)C(t)\right]\right\}. \tag{8}$$

Here, the factor $b_k(0)$ is the integral constant, and $S(t)$ and $C(t)$ are defined as

$$S(t) = \sum_{n=-\infty}^{+\infty}\frac{\sin(n\omega + d)t}{n\omega + d}\mathcal{J}_n\left(\frac{K}{\omega}\right), \tag{9}$$

$$C(t) = \sum_{n=-\infty}^{+\infty}\frac{\cos(n\omega + d)t - 1}{n\omega + d}\mathcal{J}_n\left(\frac{K}{\omega}\right), \tag{10}$$

where $\mathcal{J}_n$ denotes the $n$th ordinary Bessel function.

The analytical solutions $\alpha_m$ for the interaction-free case ($g = 0$) can be directly obtained through the inverse Fourier transform. They are the starting points to derive the trial solutions for the $g \neq 0$ case. Specifically, we are concerned with the $b_k(0) = \delta_{k,p}$ case, which can simplify the final expressions of solutions of equations (2) as

$$\alpha_m(t) = \exp\left\{\mathrm{i}m\left[p - \mathrm{d}t - \frac{K}{\omega}\sin(\omega t)\right]\right\} \times \exp\{\mathrm{i}2J[\cos(p)S(t) - \sin(p)C(t)] - \mathrm{i}gt\}. \tag{11}$$

Note that the solutions are applicable for $L \to \infty$.

To explore the dynamical stability of the system, we assume small fluctuations around the stationary solutions following the usual ansatz [13, 15], i.e. $\alpha_m(t) = \alpha_m^0(t) + \delta\alpha_m(t)$, where $\alpha_m^0(t)$ take the expressions as equations (11). The fluctuations can be expressed as

$$\delta\alpha_m(t) = \alpha_m^0(t)[u(t)\,\mathrm{e}^{\mathrm{i}qm} + v^*(t)\,\mathrm{e}^{-\mathrm{i}qm}]. \tag{12}$$

Here, $q$ is the momentum of the excitation relative to the condensates. Substituting the trial solutions into equations (2), we obtain the Bogoliubov–de Gennes (BdG) equations for the quasiparticle excitations $u(t)$ and $v(t)$:

$$\mathrm{i}\frac{\mathrm{d}}{\mathrm{d}t}\begin{pmatrix}u(t)\\v(t)\end{pmatrix} = \mathcal{M}(q,t)\begin{pmatrix}u(t)\\v(t)\end{pmatrix}, \tag{13}$$

where the elements of the matrix $\mathcal{M}(q,t)$ are given by

$$\mathcal{M}_{11}(q,t) = 4J\sin\left(\frac{q}{2}\right)\sin\left(\frac{q}{2} + p - \frac{K}{\omega}\sin(\omega t) - \mathrm{d}t\right) + g,$$

$$\mathcal{M}_{12}(q,t) = g = -\mathcal{M}_{21}(q,t),$$

$$\mathcal{M}_{22}(q,t) = 4J\sin\left(\frac{q}{2}\right)\sin\left(\frac{q}{2} - p + \frac{K}{\omega}\sin(\omega t) + \mathrm{d}t\right) + g.$$

Note that the matrix $\mathcal{M}(q,t)$ is also time-periodic with the periodicity $T$ being the lowest common multiple of $2\pi/\omega$ and

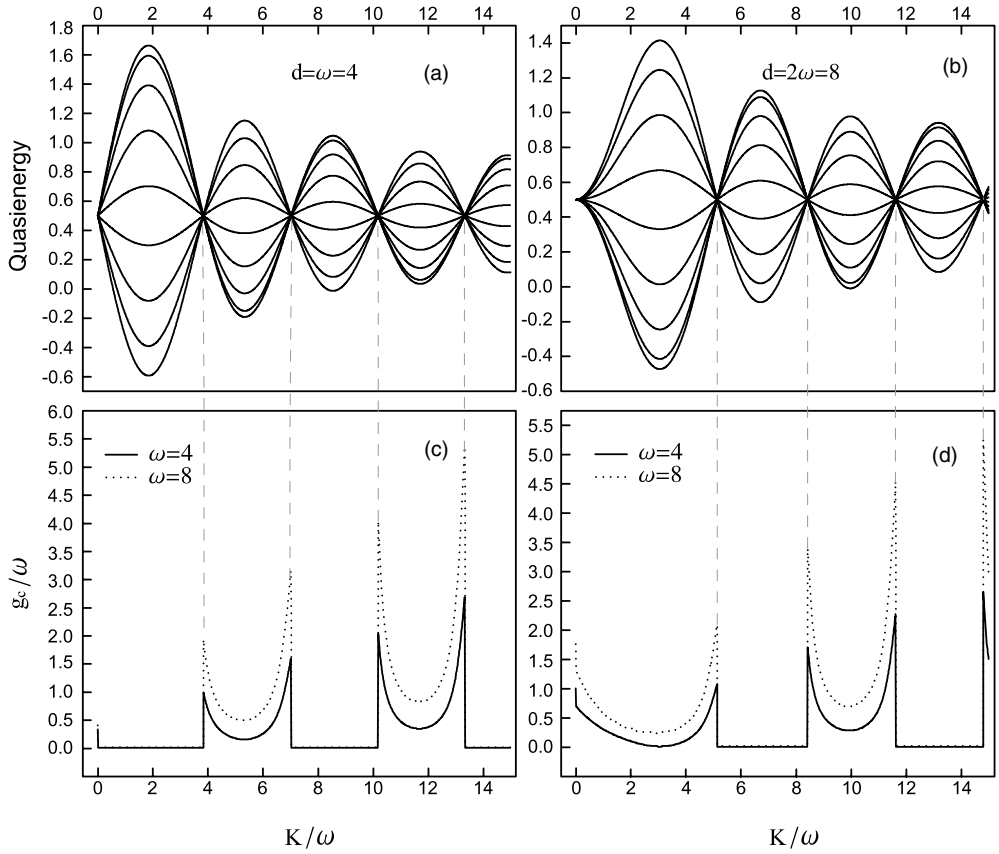


**Figure 1.** Quasienergy spectrum of a nine-site system for (a) $l = 1$ and (b) $l = 2$ and the $K/\omega$ dependence of the critical interaction $g_c$ for (c) $l = 1$ and (d) $l = 2$. The displacement of the quasienergy spectrum is $g = g' = 0.5$ for both cases. The vertical dashed lines are guides to the eye.

$2\pi/d$. Our analysis relies on the periodicity of the evolution matrix. One point we need to mention is that for irrational $d/\omega$, the matrix $\mathcal{M}(q,t)$ is quasi-periodic and the method below may become ineffective, which is beyond the scope of this paper.

It will be convenient to introduce the evolution operator $U(t)$ in order to characterize the evolution of $u(t)$ and $v(t)$, i.e. $(u(t), v(t))^T = U(t)(u(0), v(0))^T$. Thus, the dynamical behaviour $U$ is governed by

$$\mathrm{i}\frac{\mathrm{d}}{\mathrm{d}t}U(t) = \mathcal{M}(q,t)U(t). \tag{14}$$

Using the $2 \times 2$ unit matrix as the initial data, we numerically solve equation (14) over period $T$. According to the Floquet theorem, the eigenvalues $\lambda_i$ of $U(T)$ correspond to the excitation quasienergies $\varepsilon_i$ via $\lambda_i = \exp[-\mathrm{i}\varepsilon_i T]$ $(i = 1, 2)$. The dynamical stability of the system is specified by the fact that both the quasienergies $\varepsilon_i$ have no imaginary components, i.e. $|\lambda_i| = 1$. If this is so for all values of $q$, then the solution is stable; otherwise, the system may collapse. The analysis of those features can help us to map out the stability diagrams of the system in the parameter space of $g/\omega$ and $K/\omega$ which are shown in section 4.

## 3. Quasienergy

Quasienergies are closely related to the dynamical stability. Since the periodicity of the time-periodic evolution matrix in equations (4) is $T$, the Floquet theorem enables us to write the solution in the form of $\exp[-\mathrm{i}\epsilon t]\psi(t)$, where $\epsilon$ corresponds to the quasienergy of the system and $\psi(t)$ corresponds to the Floquet state which shares the same periodicity $T$. In order to obtain the quasienergies, we pick out all terms which are not $T$-periodic from $\alpha_m(t)$. Note that $g = n\omega + g'$, where $n$ is a positive integer to ensure $0 \leqslant g' < \omega$. Considering the possible divergence in the denominators of summations in $S(t)$ and $C(t)$, we analyse, separately, the cases of $l = d/\omega$ being integer and non-integer (assumed to be rational).

For integer $l$, in the limit of $d \to l\omega$, both $\exp[\sin(-l\omega + d)t/(-l\omega + d)] \to t$ and $\exp[-\mathrm{i}g't]$ are not $T$-periodic; then we have the quasienergies expressed as

$$\epsilon(p) = -2J\cos(p)\mathcal{J}_{-l}\left(\frac{K}{\omega}\right) + g'. \tag{15}$$

The situation of $d = 0$ has already been studied in [13], so here we discuss the more general case $d \neq 0$. Throughout this paper, the tunnelling strength $J$ is set to unity. As examples, we show the quasienergy spectrum for $d = \omega$ and $d = 2\omega$ in figures 1(a) and (b), respectively. The spectrum is obtained by the fundamental matrix method, which requires the diagonalization of $\vec{\alpha}(0)^T\vec{\alpha}(T)$, where $\vec{\alpha}(t) = \{\alpha_1(t), \alpha_2(t), \ldots, \alpha_L(t)\}$. As $L \to \infty$, the results match the analytical expressions (15) perfectly. Another numerical way to obtain the quasienergies is to evolve the time-evolution operator of $\vec{\alpha}(t)$ directly and diagonalize it, which yields the

same results. It is obviously observed from figures 1(a) and (b) that the spectrum is wholly displaced by the amount of $g'$, as stated above. The collapse points of the spectrum correspond to the zeros of $\mathcal{J}_{-l}(K/\omega)$, which manifests the phenomenon of coherent destruction of tunnelling. Interestingly, for nonzero $l$, in the limit of weak modulation, i.e. $K/\omega \to 0$, the tunnelling is frozen. As $K/\omega$ increases from zero to the first maximum of $\mathcal{J}_{-l}(K/\omega)$, the mobility of the condensate is enhanced. This phenomenon is called photon-assisted tunnelling which was not discussed in [13].

For non-integer $l$, the case is much simpler since all terms in $\alpha_m(t)$ have periodicity $T$ except $\exp[-\mathrm{i}g't]$. One can obtain that the quasienergies of the system are $\epsilon(p) = g'$, independent of the value of $K/\omega$. Our numerical calculations further confirm our analysis.

## 4. Dynamical stability

We are interested in the dynamical stability of the system around the ground state. As we know, for positive tunnelling strength, the momentum of the ground state is located at $p = 0$ (the center of the Brillouin zone). For negative tunnelling strength, we may extract a phase factor of $\exp[\mathrm{i}\pi]$ and consequently, the $p = \pi$ state (the edge of the Brillouin zone) has the lowest energy. We first consider the $p = 0$ state and then extend our analysis to the $p = \pi$ case when necessary.

To determine the critical interaction $g_c$ beyond which the system becomes unstable, we set all other parameters fixed and increase the value of $g$ from zero gradually for each $K/\omega$ until the unstable region is reached. Then we are able to plot the boundary between stable and unstable regions in the parameter space of $g/\omega$ and $K/\omega$.

Since equation (14) can be solved analytically when $g = 0$, it is easy to find that the excitation quasienergies are all real such that the system is always stable regardless of the value of $K/\omega$. As $g$ increases, unstable regions emerge. We observe different stability diagrams for integer and non-integer $l$.

For the case of integer $l$, we plot the stability diagrams for $l = 1$ and $l = 2$ in figures 1(c) and (d), respectively. It is clear that the dependence of $g_c$ on $K/\omega$ shows two kinds of behaviours, whose shapes seem to be alternately plateau and upward concave. We note that the separations between the two behaviours appear at the collapse points of the quasienergy spectrum, also the zeros of $\mathcal{J}_{-l}(K/\omega)$. From equation (15) we may define the effective tunnelling strength $J_{\mathrm{eff}}(K/\omega) = J\mathcal{J}_{-l}(K/\omega)$, while the flat critical interaction regions ($g_c \to 0$) correspond to the negative effective tunnelling strength ($J_{\mathrm{eff}} < 0$) with repulsive interaction ($g > 0$). As we know, for positive inter-well tunnelling strength in the typical Bose–Hubbard model, attractive interaction may induce the collapse of BEC [20]. In analogy with it, due to the symmetry of the system Hamiltonian [21], a minus sign can be extracted without affecting the physics. We may draw the conclusion that for negative effective tunnelling strength ($J_{\mathrm{eff}} < 0$), no positive interaction can stabilize the system. When $J_{\mathrm{eff}}(K/\omega) = 0$, coherent destruction of tunnelling occurs, freezing the dynamics of the system, thus favouring the stability. As a result, $g_c$ peaks around these critical points where the phenomenon of self-trapping may occur, physically speaking. Between the zeros of Bessel functions, photon-assisted tunnelling increases the mobility of the condensate, forming the upward concaves as we have observed.

The complete instability for the negative effective tunnelling strength can also be interpreted from another point of view. When $J_{\mathrm{eff}} < 0$, $p = 0$ is no longer the ground state, but the most excited state with the highest energy which causes the unstable behaviour. Since we are concerned with the dynamical properties of the ground state, we need to consider the $p = \pi$ state when $J_{\mathrm{eff}} < 0$. As an example, we plot the stability diagram of the exact ground state for $l = 1$ in figure 2(a). Around the zero points of the Bessel function $\mathcal{J}_{-1}(K/\omega)$, the effective tunnelling strength $J_{\mathrm{eff}}$ changes its sign, inducing the sudden switch of the ground state from $p = 0$ to $p = \pi$ and vice versa. However, the critical interaction strength varies continuously.

As a demonstration of dynamical instability, we show the evolution behaviour of the ground state in figures 2(b) and (c). Equation (11) with $p = 0$ is considered as the initial state and the evolution is restricted to a nine-site system. The difference between equation (11) and the exact solution for the few-site lattice system can be viewed as the perturbation. When the interaction $g$ is less than $g_c$, during the evolution the system is always stable, as shown in figure 2(b). On the other hand, when $g > g_c$, the perturbation can drive the system into chaotic evolution, as shown in figure 2(c).

As we have observed, for some $l$, e.g., $l = 1$, as $K \to 0$, the critical interaction strength $g_c$ coincides with that of $K = 0$, as shown in figure 2(a). However, for other nonzero $l$ there exists a finite mismatch between them, as shown in figure 1(d). This is quite different from the $l = 0$ ($d = 0$) case studied in [13] in which the author observed a divergence of $g_c$ at $K = 0$ and a sharp transition when $K \to 0$. When there is no time-periodic modulation, i.e. $K = 0$, we observe the nonzero critical interaction strength $g_c$ which coincides with experimental data [14]. For trapped $^{87}$Rb gases, the tunnelling strength is approximately $2\pi \times 1700$ Hz; the interaction strength is about $2\pi \times 94$ Hz; and the constant acceleration forces are $2\pi \times 26$ Hz, $2\pi \times 43$ Hz, $2\pi \times 85$ Hz and $2\pi \times 425$ Hz. The first three experimental points are unstable while the last one is stable. In our theory, when the tunnelling strength is set to be the unit, i.e. $J = 1$, then we have $g = 0.11$, $d = 0.03$, 0.05, 0.1 and 0.5. For each value of $d$, we can calculate the corresponding $g_c$ as 0.01, 0.019, 0.037 and 0.17. Comparing them with the value of $g$, we can confirm our theoretical results which agree with [15].

We also note the recent experiment [17] of photon-assisted tunnelling whose model is exactly the same as ours. About $10^4$ $^{87}$Rb atoms were trapped and the tunnelling properties were investigated. The tunnelling strength is $J = 2\pi \times 270$ Hz and the acceleration force is $d = 2\pi \times 380$ Hz. Two modulation frequencies are chosen to be $\omega = 2\pi \times 380$ Hz ($l = 1$) and $2\pi \times 190$ Hz ($l = 2$), corresponding to $\omega/J = 1.4$ and 0.7, respectively. In both cases, the critical interaction strengths $g_c$ approach zero when $K/\omega$ is

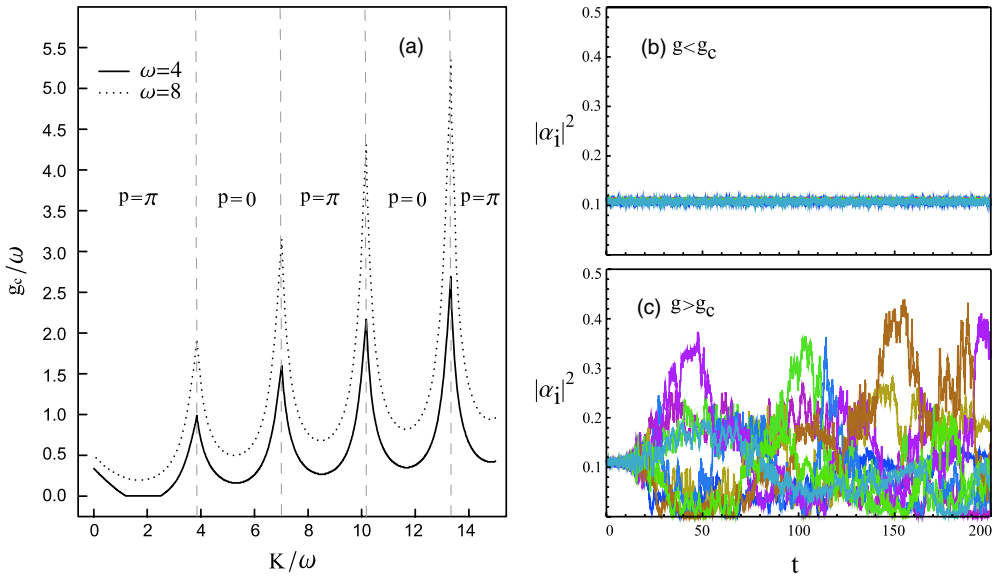


**Figure 2.** (a) The $K/\omega$ dependence of the critical interaction $g_c$ for $l = 1$ at the driving frequencies $\omega = 4$ (solid line) and $\omega = 8$ (dotted line). Based on the sign of $J_{\text{eff}}$, the instability analysis is made about different Floquet states (labelled as $p = 0$ and $p = \pi$). The time evolution of population probabilities $|\alpha_i|^2$ in a nine-site system for (b) $g/\omega = 0.5$ and (c) $g/\omega = 1.5$. The initial state is chosen to be equation (11) with $p = 0$, and other parameters are $\omega = 8$, $K/\omega = 10$ and $l = 2$. In this case $g_c/\omega \approx 0.7$. $1/J$ is the unit of time. In (b) and (c) stable and unstable evolution behaviours are observed, respectively.

away from the zeros of Bessel functions around which $g_c$ is comparable to the value of $\omega/J$. In the experiment the interaction strength is about $g = 2\pi \times 10$–$2\pi \times 30$ Hz; we can estimate that $g/\omega = 0.026$–$0.158$ which is above zero, however, smaller than the value of $g_c$ near the zeros of Bessel functions. This is why the experimental data fit theory is better when the value of $K/\omega$ is near the zeros of Bessel functions than when away from them. The authors also argued that the better agreement between the experimental data and the squares of the Bessel functions rather than their moduli could be explained by sequential tunnelling requiring a dephasing mechanism which corroborates with our dynamical instability analysis. We suggest increasing the value of $\omega$ to stabilize the system which may enhance the agreement between experiment and theory. Besides, to account for the detailed time dependence of the condensate expansion is also expected to improve the theoretical description of experimental results [23].

For the case of non-integer $l$, we start our analysis about the $p = 0$ state with the half-integer $l$ case. As an example, we plot the stability diagram for $l = 0.5$ in figure 3(b). As discussed in section 3, the quasienergies for non-integer $l$ are $g'$, independent of the value of $K/\omega$. As a result, no correspondence between the quasienergies and $g_c$ peaks is observed, as expected. In order to determine the positions of $g_c$ peaks approximately, we have to resort to the expression of $\alpha_m(t)$. Since the summations appear in the exponent of equation (11), as $|n + l|$ increases, the contribution from the $n$th term reduces rapidly, if the high modulation frequency limit is assumed, i.e. $\omega \gg 1/J$ [22]. The dominant terms would be those with the smallest values of $|n + l|$. As an example, for $l = 0.5$, the dominant contributions to $\alpha_m(t)$ would come from $\mathcal{J}_0(K/\omega) + \mathcal{J}_{-1}(K/\omega)$ which is plotted in figure 3(a). The correspondence between the zeros and $g_c$ peaks is observed, confirming our analysis. As stated before, the dynamics of the system is frozen at the zeros of Bessel

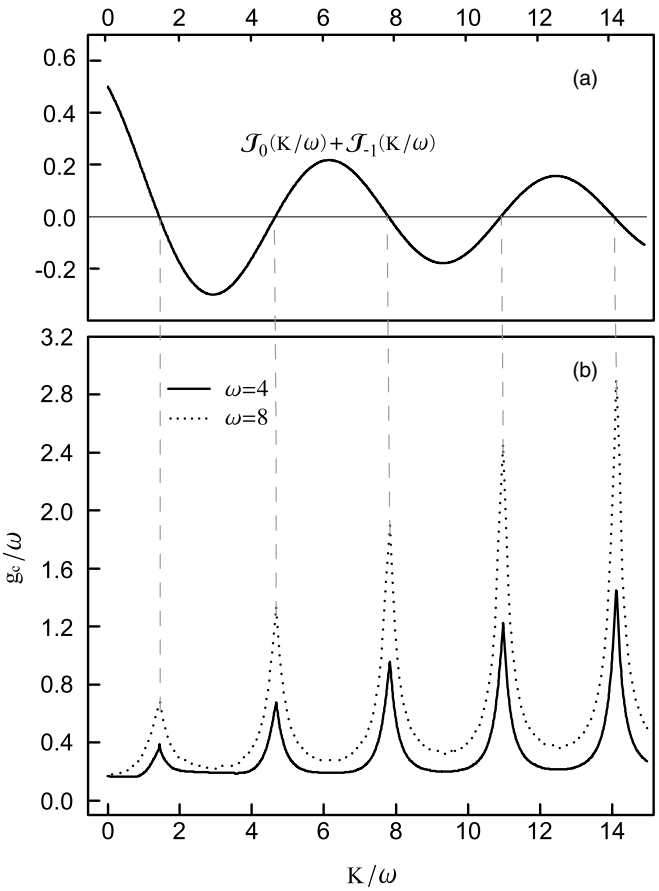


**Figure 3.** The $K/\omega$ dependence of (a) $\mathcal{J}_0(K/\omega) + \mathcal{J}_{-1}(K/\omega)$ and (b) the critical interaction $g_c$ for $l = 0.5$. The vertical dashed lines are guides to the eye.

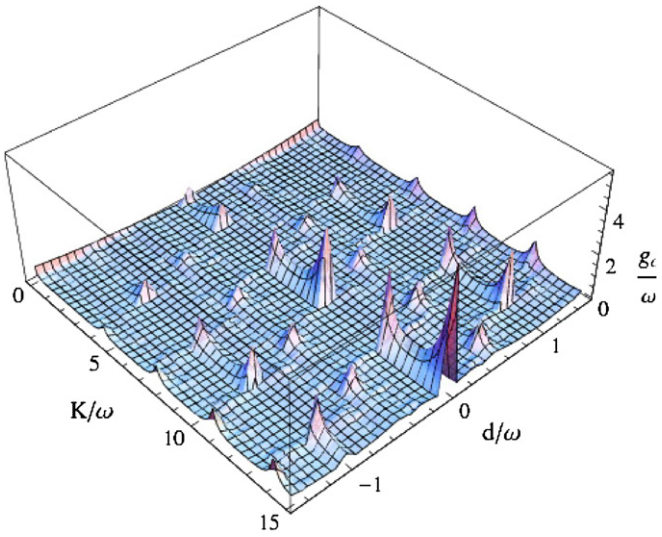


**Figure 4.** Dependence of the critical interaction $g_c$ on $K$ and $d$ for $-1.5 \leqslant l \leqslant 1.5$ in the case of $\omega = 4$.

functions, indicating the appearance of stable regions, where $g_c$ peaks with the greatest probability. We also note the whole displacement of $g_c$ which depends on $d$. In figure 4 we plot the behaviours of dynamical stability around integer and half-integer $l$, compared with which the crossover between them shows no explicit dependence of $g_c$ on the values of $K/\omega$. We may interpret the behaviour as the counterbalance of different Bessel functions. Also from figure 4, we can find the same dependence of $g_c$ on $d$ as found in [16] without time-periodical modulation, i.e. $K/\omega = 0$.

Additionally, for both integer and non-integer $l$, we find that the bigger value of $\omega$ favours the high modulation frequency limit, and also enhances the dynamical stability of the system as shown in figures 1(c), 1(d), 2(a) and 3(b).

## 5. Summary

We considered the system of BEC in one-dimensional tilted time-periodically modulated lattices. The ratio $l$ of the acceleration force $d$ to the modulation frequency $\omega$ is defined to help divide our analysis into integer and non-integer resonances. Due to the time periodicity of the system Hamiltonian, we gave the explicit expressions of quasienergies for both cases referring to integer and non-integer (rational) resonances by making use of the Floquet theorem. For integer $l$, the quasienergy spectrum shows its correspondence to the Bessel function $\mathcal{J}_{-l}(K/\omega)$ whose zeros correspond to the collapse points of the spectrum, indicating the appearance of coherent destruction of tunnelling. However, for non-integer $l$, no dependence of the quasienergies on $K/\omega$ is found.

We investigated the dynamical stability of the system more around the ground state by characterizing it in the parameter space of the interaction strength and the modulation amplitude. For the $p = 0$ state, when $l$ is integer, we observed two alternate behaviours of the dependence of the critical interaction strength $g_c$ on $K/\omega$: plateau ($g_c \to 0$) and upward concave. The complete instability in horizontally flat regions is brought out by the negative effective tunnelling strength. The separations between the two kinds of regions correspond to the zeros of the Bessel function $\mathcal{J}_{-l}(K/\omega)$.

Since the ground state is the $p = \pi$ state, not the $p = 0$ state for the negative tunnelling strength, we made a comparative instability analysis on the $p = \pi$ state when $J_{\text{eff}} < 0$. Around the zeros of the Bessel function $\mathcal{J}_{-l}(K/\omega)$ continuous behaviour is observed. We also found that the bigger value of $\omega$ favours the stability of the system. Additionally, we numerically simulated the time evolution of the ground state in a nine-site lattice. Different behaviours for $g < g_c$ and $g > g_c$ confirm the boundary of the critical interaction strength between stable and unstable regions.

In our calculation, as $K \to 0$, the critical interaction strength coincides with that of $K = 0$. This is quite different from the $d = 0$ case studied in [13] where a divergence of $g_c$ and a sharp transition at $K = 0$, were observed. We also compared our results with experimental data where a perfect agreement for the $K = 0$ case [14] is observed. The experiment of photon-assisted tunnelling for $l = 1$ and $l = 2$ [17] confirms our analysis for the $K > 0$ case.

Among non-integer resonances, we observed that $g_c$ peaks are centered around the half-integer $l$ for which the completely unstable regions disappear ($p = 0$ case). Also the whole displacement of $g_c(K/\omega)$ emerges whose value is dependent on $d$. The positions of $g_c$ peaks in the direction of $K/\omega$ are determined approximately in the high modulation frequency limit. The large driving frequency $\omega$ enhances the dynamical stability of the system. Compared with integer and half-integer resonances, the crossovers between them show no explicit dependence of $g_c$ on the modulation amplitude.

Bose–Einstein condensates in optical lattices have received much attention in recent years where stability analysis plays an important role. Since dynamical instability is experimentally observable, these features are expected to be examined directly in real systems. Our analysis could help experimentalists to avoid the unwanted or target the desired regions in parameter space.

## Acknowledgment

The work is supported by NSFC grant no 10874149 and partially by PCSIRT grant no IRT0754.

## References

[1] Anderson M H, Ensher J R, Matthews M R, Wieman C E and Cornell E A 1995 *Science* **269** 198
[2] Bradley C C, Sackett C A, Tollett J J and Hulet R G 1995 *Phys. Rev. Lett.* **75** 1687
[3] Davis K B, Mewes M-O, Andrews M R, van Druten N J, Durfee D S, Kurn D M and Ketterle W 1995 *Phys. Rev. Lett.* **75** 3969
[4] Greiner M, Mandel O, Esslinger T, Hänsch T W and Bloch I 2002 *Nature* **415** 39
[5] Creffield C E and Monteiro T S 2006 *Phys. Rev. Lett.* **96** 210403
[6] Sias C, Zenesini A, Lignier H, Wimberger S, Ciampini D, Morsch O and Arimondo E 2007 *Phys. Rev. Lett.* **98** 120403
[7] Morsch O, Müller J H, Cristiani M, Ciampini D and Arimondo E 2001 *Phys. Rev. Lett.* **87** 140402

[8] Eckardt A, Holthaus M, Lignier H, Zenesini A, Ciampini D, Morsch O and Arimondo E 2009 *Phys. Rev.* A **79** 013611
[9] Wu B and Niu Q 2001 *Phys. Rev.* A **64** 061603
[10] Wu B and Niu Q 2003 *New J. Phys.* **5** 104
[11] Fallani L, De Sarlo L, Lye J E, Modugno M, Saers R, Fort C and Inguscio M 2004 *Phys. Rev. Lett.* **93** 140406
[12] Lignier H, Sias C, Ciampini D, Singh Y, Zenesini A, Morsch O and Arimondo E 2007 *Phys. Rev. Lett.* **99** 220403
[13] Creffield C E 2009 *Phys. Rev.* A **79** 063612
[14] Cristiani M, Morsch O, Malossi N, Jona-Lasinio M, Anderlini M, Courtade E and Arimondo E 2004 *Opt. Exp.* **12** 4
[15] Zheng Y, Koštrun M and Javanainen J 2004 *Phys. Rev. Lett.* **93** 230401
[16] Kolovsky A R, Korsch H J and Graefe E M 2009 *Phys. Rev.* A **80** 023617
[17] Sias C, Lignier H, Singh Y P, Zenesini A, Ciampini D, Morsch O and Arimondo E 2008 *Phys. Rev. Lett.* **100** 040404
[18] Eckardt A, Jinasundera T, Weiss C and Holthaus M 2005 *Phys. Rev. Lett.* **95** 200401
[19] Kolovsky A R and Korsch H J 2009, arXiv:cond-mat/0912.2587v2
[20] Pattanayak A K, Gammal A, Sackett C A and Hulet R G 2001 *Phys. Rev.* A **63** 033604
[21] Myatt C J, Burt E A, Ghrist R W, Cornell E A and Wieman C E 1997 *Phys. Rev. Lett.* **78** 586
[22] Creffield C E 2003 *Phys. Rev.* B **67** 165301
[23] Creffield C E, Sols F, Ciampini D, Morsch O and Arimondo E 2010, arXiv:cond-mat/1008.0709v1